Journal of Manufacturing Processes 32 (2018) 77–84

Contents lists available at ScienceDirect

Journal of Manufacturing Processes

journal homepage: www.elsevier.com/locate/manpro

Thermodynamic analysis of the aluminum alloy foaming process by melt route

Marlenne González-Nava[a,*], Alejandro Cruz-Ramírez[a], Miguel Ángel Suarez-Rosales[b], María de los Ángeles Hernández Pérez[a]

[a] Departamento de Ingeniería en Metalurgia y Materiales, Instituto Politécnico Nacional - Escuela Superior de Ingeniería Química e Industrias Extractivas (ESIQIE), UPALM, México D.F, 07051

[b] Instituto de Investigaciones en Materiales, UNAM, Circuito exterior s/n. Cd. Universitaria, México D.F, 04510

ARTICLE INFO

Article history:
Received 14 February 2017
Received in revised form 21 January 2018
Accepted 29 January 2018
Available online 5 February 2018

Keywords:
Metallic foams
Aluminum alloy
Compounds
Thermodynamic analysis
Foaming agent

ABSTRACT

A thermodynamic analysis was carried out to determine the stability compounds formed by the interaction between the molten alloy (A356 alloy) with a foaming agent (1, 2, 3 wt. % $CaCO_3$) and a thickening agent (1 wt. % Al_2O_3) for the production of closed-cell aluminum alloy foams. Stability phase diagrams were obtained to 973, 1073 and 1173 K and they showed the formation of the compounds $MgAl_2O_4$, $CaAl_4O_7$, Al_4C_3, and Al_4O_4C. Typical closed-cell foams of the A356 aluminum alloy were produced to the same conditions of the thermodynamic analysis. The structure of the foams produced was evaluated by SEM-EDS and Raman techniques. The stability compounds predicted are in good agreement with those determined experimentally. The compounds formed by the interaction between the particles and the melt were increased with the increase of the foaming agent and were located at the cell walls.

1. Introduction

Methods for producing metal foams are already known and classified [1,2]. Molten metal can be processed to a porous material by interacting gas into the melt [3] or by adding a foaming agent into it [4]. Most of the closed-cell aluminum foams are produced by adding a foaming agent to the molten aluminum together with stirring. TiH_2 is a popular foaming agent because of its decomposition temperature, which is close to the melting temperature of aluminum alloys. However, a particular concern is the control of pore size, porosity level, the homogeneity of the foam and high production costs. In order to meet the above requirements, a new easily available agent for metal foaming, calcium carbonate was proposed as a cheaper and safer foaming agent than the conventional agent, titanium hydride [1–6]. Lázaro et al. [7] produced aluminum alloy foams by using an alternative carbonate constituted by a mixture of magnesite and dolomite. The carbonate mixture was added from 0.7 to 5 wt. % and mixing time varied from 1 to 3 min, while stirring at 600 rpm. The foaming agent is trapped and decomposes into a gas and then dissolves into the liquid, which causes the melt to foam. Calcium carbonate gives a finer cell structure than TiH_2 in the melt route. CO_2 gas is readily available from the decomposition of carbonates, which oxidizes and stabilizes the aluminum cell surface. Thus, the aluminum foam produced using carbonates has a finer cell structure than that produced using TiH_2 [8]. In general, CO_2 is the best gas to be trapped in the pores, since it is easily obtainable, has a low thermal conductivity and low toxicity [9]. The foaming process is rather complicated because the foam formation is governed by a complex interplay between cells and the solid-liquid interface so that an unstable liquid film easily leads to bubble collapse and an imperfect foam structure is obtained. To obtain homogeneous pore distribution it is necessary to avoid drainage of aluminum melt, coarsening and rupture of cell walls during solidification, which leads to the generation of coarsened cells. Thickening agents, such as silicon carbide, aluminum oxide or other ceramic particles can be used to carry out the aluminum foaming process [10]. It was found that the foam stability can be increased by using Al_2O_3 instead of SiC, because of increased cell wall thickness [11]. An alternative way of foam generation involves adding calcium to an aluminum alloy and stirring in the presence of air which leads to an in situ creation of solid particles in the melt that increase the viscosity of the melt and suppress the drainage of aluminum melt during solidification [12].

Yang and Nakae [13] added aluminum powder to an aluminum alloy melt and found an increase in viscosity and foamability. Recently, it was reported that magnesium, which oxidizes easily, works as a thickening agent for aluminum alloys containing magnesium in its chemical composition [14]. Liquid metals, especially

* Corresponding author.
E-mail addresses: marlagn2701@hotmail.com (M. González-Nava), alcruzr@ipn.mx (A. Cruz-Ramírez), msuarez@iim.unam.mx (M.Á. Suarez-Rosales), mhernandezp0606@ipn.mx (M.d.l.Á.H. Pérez).

https://doi.org/10.1016/j.jmapro.2018.01.028
1526-6125/

aluminum form a strong, compact and thick oxide layer on the surface in an oxidizing atmosphere. Oxidizing gases and those alloying elements that increase the strength of the oxide film may increase the stability of aluminum foam melt. The accumulation of oxide particles in regions close to the surface of films increases the surface viscosity promoting slowdown drainage. Reactions between the stabilizing particles and the melt could be observed in some cases. A micrograph of an Alporas foam shows by an EDX analysis, the presence of precipitates which contain various mixed oxides of aluminum, calcium, and titanium such as Al_2CaO_4 or $Al_2Ca_3O_6$, or oxide mixes $Al_2O_3 + TiO_2$ or intermetallic compounds such as Al_4Ca, Al_2Ca or Al_3Ti [15,16]. Byakova et al. [17] studied the role of foaming agent and processing route in the formation of by products which contaminate the cell wall and affect the macroscopic mechanical response of closed-cell aluminum foams. For aluminum foams processed with calcium additive, coarse particles of the Al_2CaSi_2 intermetallic compound were observed in the cell wall. These particles reduced the compressive strength to values close or below to those of open-cell foams of the same relative density. It is evident from the literature review [1–17] that the foaming process via melt route involves reactions between the foaming and thickening agents and the melt. The products obtained from these reactions forms clustered structure which can cause faster sedimentation of the particles on the foam surface or in the metallic melts, affecting the cell wall structure and the mechanical properties of the metal foams. It has been reported that Mg in the liquid aluminum can react with Al_2O_3 producing spinel or MgO layer on its surface [18]. Babcsán [19] carried out a thermodynamic analysis to determine the minimum magnesium concentration required to form the compound $MgAl_2O_4$ in Al-10Si alloy at 1000 K. There are few research works [18,19] related to the prediction of compound formation in the manufacturing of aluminum alloy foams by melt route and its effect on the foam structure. In addition, depending on the foaming process parameters, the components can react with the melt to form different compounds that will affect the foam properties. In the present work, a thermodynamic analysis was carried out to determine the compounds formed by the interaction between the A356 aluminum alloy and the thickening (Al_2O_3) and foaming agent ($CaCO_3$) with the thermodynamic software Factsage 7.0 [20]. Stability phase diagrams were obtained at 973, 1073 and 1173 K in order to explain the foaming process and the compounds formation. The predicted compounds were compared with those obtained by the manufacture of A356 aluminum alloy foams by SEM-EDS and Raman analysis.

2. Experimental procedure

2.1. Fabrication of A356 aluminum alloy foams

A master A356 alloy was manufactured by conventional melting in a gas furnace at 1023 K from pure metals. The following chemical composition was obtained by Atomic Emission Spectrometry for the A356 aluminum alloy (92.3 wt% Al, 7.12 wt% Si, 0.38 wt% Mg, 0.2 wt % Cu). 500 g of the master alloy was set in a stainless steel crucible. The alloy was melted and kept at 1023 K in an electric furnace under atmospheric pressure. The heating system was an electrical furnace enabled with control of temperature to within ± 10 K of the set values. The temperature was measured with a K-type thermocouple. The experiments were carried out using a stir-caster system with a stainless steel paddle axle. The viscosity of the melt was modified by adding 1 wt % of Al_2O_3 (0.3 μm, 99%) of the mass charge at a constant stirring speed of 1600 rpm for 2 min. $CaCO_3$ (14 μm, 98.5%) was added as a foaming agent in amounts of 1, 2 and 3 wt % of the mass charge into the melt at a stirring speed of 1600 rpm for 100 s. After the foaming agent addition, the melt was kept in the furnace at the holding temperature of 1023 K for 2 min to allow the foam formation. The cooling procedure was carried out as soon as the expansion process took place. The crucible containing the melt was removed from the furnace and the crucible was cooled by sprayed water.

2.2. Foam characterization

The fabricated A356 aluminum foams were cut on the cross section in order to obtain samples to evaluate density and cell structure. The density and relative density of the aluminum foams were measured by weighing a sample of known volume. The cell structure was observed by optical microscopy and the image analyzer Carnoy. The microstructure examination of Al-foams and a qualitative chemical analysis of the particles formed during foaming were determined with the SEM Jeol 6300 and with the energy dispersive spectra (EDS) analysis. Images were obtained to different magnifications with backscattering electrons with 15 kV and 10 A. Room temperature Raman analysis was performed by employing a Horiba LabRAM HR Evolution spectrometer equipped with a confocal microscope. A He-Ne (632.8 nm) laser was used to excite the samples; the spot size was fixed at 20 micrometers. Spectra were recorded during 20 s with five accumulated scans.

2.3. Thermodynamic analysis

The thermodynamic analysis was carried out with the Equilib module contained in the software Factsage 7.0 [20]. Equilib was used to determine the concentration of the different chemical species once they reach the chemical equilibrium state. The user gives the initial amount of chemical species, the temperature and the pressure of the system (usually 1 atm), then the program calculates the most stable species with the Gibbs free energy minimization method. The thermodynamic analysis was carried out considering the following system: $[Al\text{-}Mg]_{alloy}$-$(aAl_2O_3)_{thickening\ agent}$-$(bCaCO_3)_{foaming\ agent}$. Where a and b values were set in the range from 0 to 1 wt% and 0 to 3 wt%, respectively.

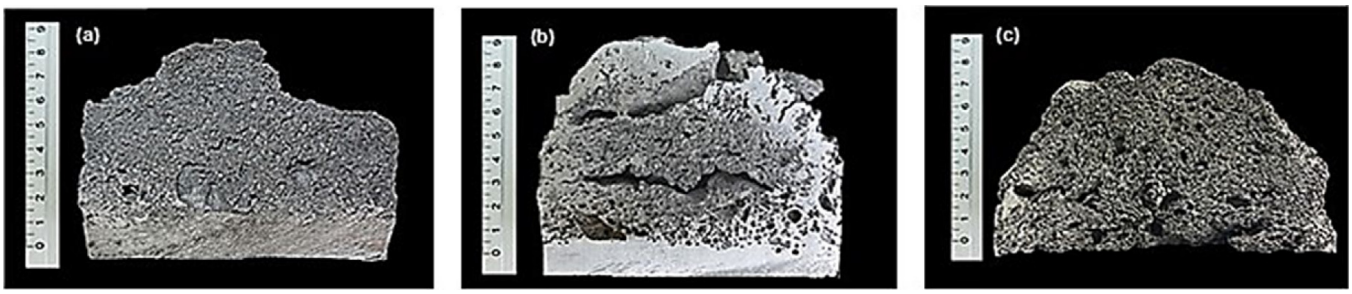

Fig. 1. Structure of the A356 aluminum alloy foams manufactured to the foaming additions of a) 1 wt% $CaCO_3$, b) 2 wt% $CaCO_3$ and c) 3 wt% $CaCO_3$ using Al_2O_3 as a foaming agent.

Fig. 2. A356 aluminum alloy foams manufactured to the foaming additions of (a) 1 wt % $CaCO_3$, (b) 2 wt % $CaCO_3$ and (c) 3 wt % $CaCO_3$.

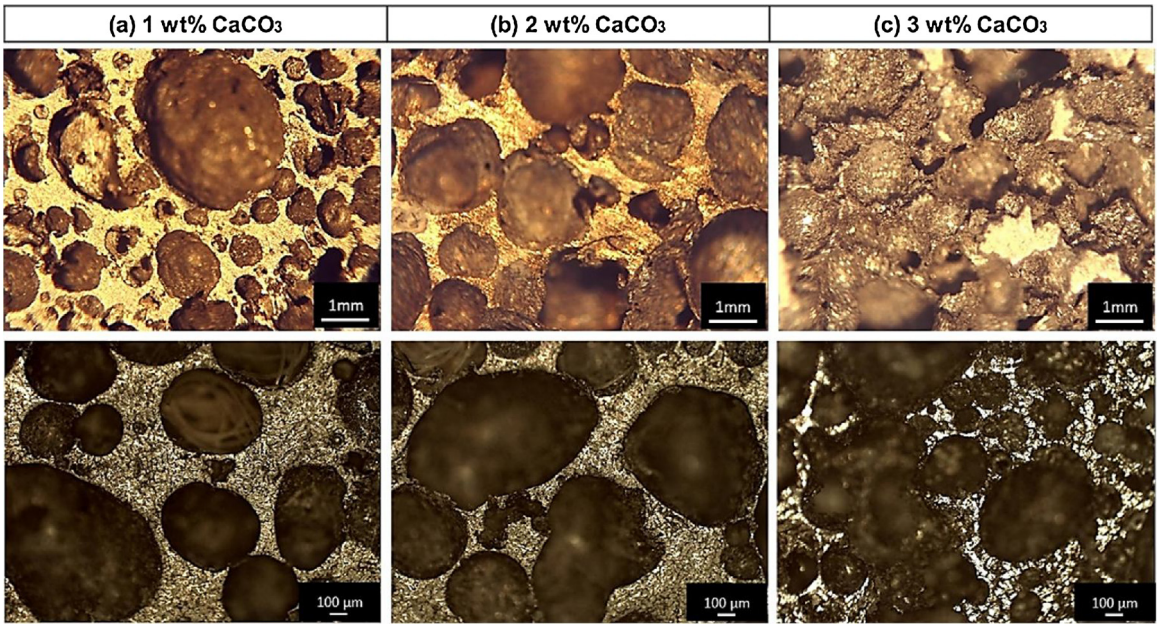

Fig. 3. Stereoscopic and Microscopic analysis of A356 aluminum alloy foams manufactured to the foaming additions of (a) 1 wt % $CaCO_3$, (b) 2 wt % $CaCO_3$ and (c) 3 wt % $CaCO_3$.

The database used for the analysis does not contain silicon and copper, therefore, these metals were not considered in the alloy chemical composition. The compounds predicted were obtained at 973, 1073 and 1173 K and 1 atm.

3. Results

3.1. Cell structure

The foams and their cross-sectional views are shown in Fig. 1. The foam obtained with 1 wt % $CaCO_3$ (Fig. 1a) shows almost a homogeneous pore structure in shape and size. Fig. 1b shows the foam produced with 2 wt % $CaCO_3$, it is observed cracks in the whole foam and some solid areas. The foam obtained with 3 wt % $CaCO_3$ shows a lower expansion and low stability decreasing it is cell amount. The foam stability behavior is attributed to the interaction of the particles with the gas-liquid interfaces. It was observed a high oxidation on the top part of the melt, affecting the stability and the expansion of the foam. In order to have stable liquid-aluminum foam, both a suitable amount of poor wetting particles and a sufficiently thick oxide layer are necessary [19].

Typical closed-cell A356 aluminum alloy foams were produced by adding $CaCO_3$ as a foaming agent. The aluminum foam density (ρ^*) was determined by a volumetric method considering the weight and the geometry of the cylindrical samples shown in Fig. 2. The relative density (ρ_{Rel}) was obtained from the ratio between the aluminum foam density and the metal matrix density ($\rho_{A356} = 2.56\ g\ cm^{-3}$). The porosity (Pr %) of the A356 aluminum foams was calculated according to Eq. (1).

$$Pr(\%) = (1-\rho^*/\rho_{A356})100 \quad (1)$$

The cell structures of the foams were observed by stereoscopy and optical microscopy, the results of which are shown in Fig. 3. It is observed that the cells of the foam are essentially hemispherical and partially closed with a wide size pore distribution. The cell size was measured with the image analyzer Carnoy. Table 1 summarizes the results of density, relative density, porosity and the cell size range for the foams obtained to different $CaCO_3$ amounts.

3.2. Experimental compounds formation

Fig. 4, 5 and 6 show SEM micrographs and EDS analysis of the compounds formed in the A356 alloy foams with the addition of 1,

Table 1
Experimental densities, porosity and cell size of the A356 alloy foams.

Sample	Density ρ^* (g cm^{-3})	Relative density $\rho^*/\rho_{A356\ alloy}$	Pr (%)	Cell Size range (mm)
1 wt % $CaCO_3$	0.3859	0.1507	84	0.46–0.69
2 wt % $CaCO_3$	0.5730	0.2237	77	0.35–0.65
3 wt % $CaCO_3$	0.7154	0.2793	72	0.30–0.45

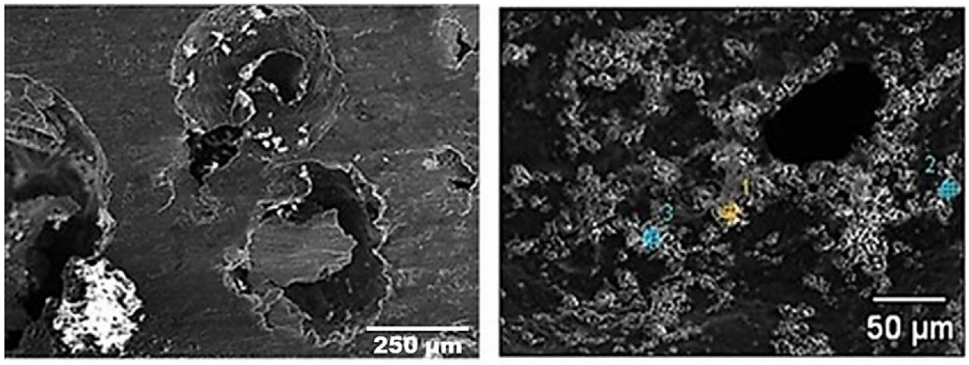

Point	Composition (wt%)	Compound
1	$Al_{41.53}O_{35.68}Ca_{22.62}C_{0.17}$	$CaAl_4O_7$
2	$Al_{53.07}O_{34.56}C_{10.94}Si_{0.95}Cu_{0.48}$	Al_4O_4C
3	$Al_{56.55}O_{41.07}Ca_{2.38}$	Al_2O3 + Ca particles

Fig. 4. SEM micrographs of the A356 aluminum alloy foam obtained to 1 wt % $CaCO_3$.

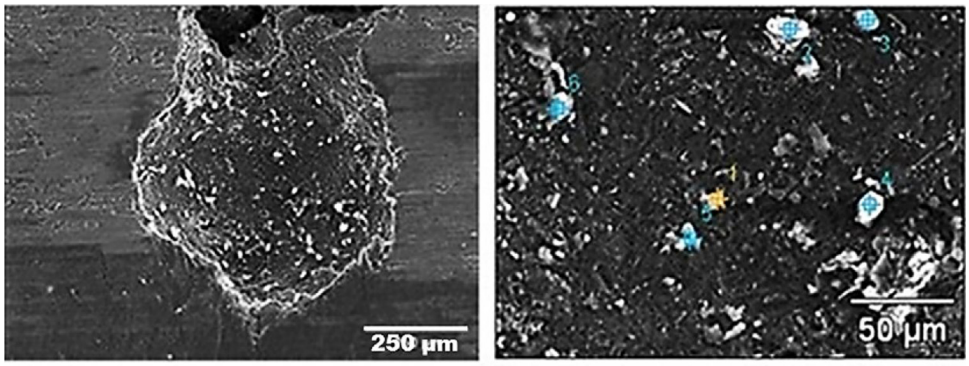

Point	Composition (wt%)	Compound
1	$Al_{44.84}O_{39.91}Ca_{14.53}Mg_{0.41}Fe_{0.31}$	$CaAl_4O_7$
2	$Al_{0.53}O_{43.19}C_{12.68}Ca_{32.34}Sr_{8.66}Ba_{2.60}$	$CaCO_3$
3	$Al_{2.87}O_{42.44}C_{11.82}Ca_{30.25}Sr_{6.81}Ba_{5.81}$	$CaCO_3$
4	$Al_{1.70}O_{37.20}C_{17.33}Ca_{33.95}Sr_{7.80}Ba_{1.96}$	$CaCO_3$
5	$Al_{58.72}O_{32}C_{9.28}$	Al_4O_4C
6	$Al_{61.38}O_{32.34}C_{6.28}$	Al_4O_4C

Fig. 5. SEM micrographs of the A356 aluminum alloy foam obtained to 2 wt % $CaCO_3$.

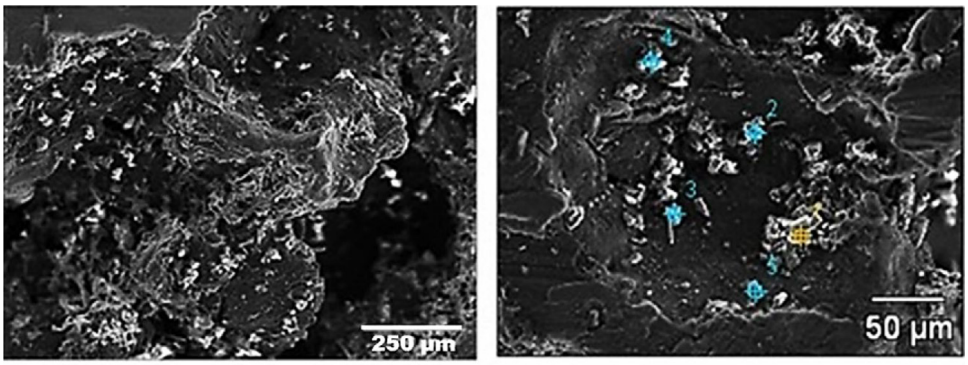

Point	Composition (wt%)	Compound
1	$Al_{78.37}O_{1.92}C_{19.35}Si_{0.36}$	Al_4C_3
2	$Al_{57.68}O_{34.82}C_{7.5}$	Al_4O_4C
3	$Al_{0.66}O_{30.96}C_{15.94}Ca_{52.44}$	$CaCO_3$
4	$Al_{60.18}O_{32.54}C_{7.28}$	Al_4O_4C
5	$Al_{73.97}O_{1.38}C_{23.87}Si_{0.70}$ $Ca_{0.08}$	Al_4C_3

Fig. 6. SEM micrographs of the A356 aluminum alloy foam obtained to 3 wt % $CaCO_3$.

2 and 3 wt % $CaCO_3$, respectively. The SEM micrographs show the presence of small particles and aggregates randomly scattered in the cell walls. The qualitative chemical analysis obtained by EDS for the foams manufactured to 1, 2 and 3 wt% $CaCO_3$ show that these foreign particles in the aluminum foams produced correspond to compounds such as Al_4O_4C, Al_4C_3, $CaAl_4O_7$ and, $CaCO_3$. Small amounts of elements as Mg, Si, Sr and, Ba were detected, which belong to the matrix alloy.

Fig. 4 shows the compounds formed with the addition of 1 wt % $CaCO_3$; the presence of Al_2O_3, $CaAl_4O_7$ and, Al_4O_4C is observed. When the $CaCO_3$ amount was increased to 2 and 3 wt%, the same compounds and, unreacted calcium carbonate were observed. A high concentration of particles attached to the cell wall is observed for the higher additions of the foaming agent.

Fig. 7 presents Raman spectra of the metallic and cell wall zone of the A356 aluminum alloy foams with different $CaCO_3$ wt% addition; an image of both zones is inset in Fig. 7. To all samples, the spectrum of the metallic zone is the same and it does not present any signal in the explored range. However, the spectra of the foams, obtained from the cell wall zone, show an intense and well defined characteristic peak around 517 cm^{-1} which is assigned to Al_4O_4C [21], this compound was identified by EDS. Other low-intensity signals of the same compound are present at 299, 430 and 990 cm^{-1}. Small and broad signals perceived to 2 wt% $CaCO_3$ foam agree to Al_4C_3 [22], $CaAl_4O_7$ [23] and $MgAl_2O_4$ [24]. The peaks observed at 278, 712 and 1085 cm^{-1} correspond to calcite [25] Raman shift and these signals are present with very high intensity in the foam prepared with 3 wt% $CaCO_3$, which indicates a high quantity of $CaCO_3$ on the cell wall and match with EDS analysis.

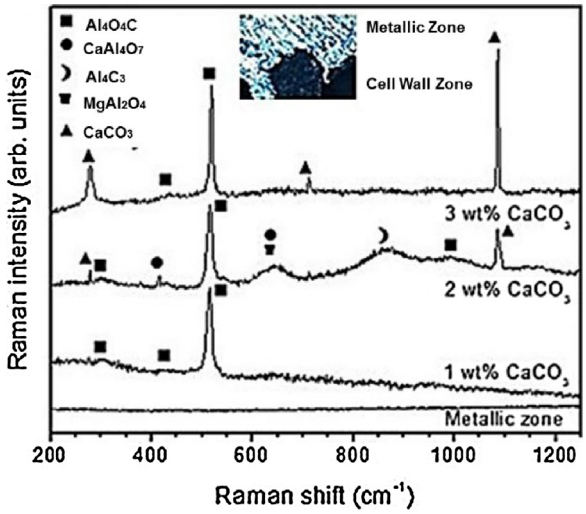

Fig. 7. Raman spectra of the A356 aluminum alloy foams obtained to 1, 2 and 3 wt. % $CaCO_3$.

3.3. Thermodynamic analysis

Equilib was used to determine the concentration of the different chemical species once they reach the chemical equilibrium state.

Fig. 8 shows the stability phase diagram at 973 K. It is observed two main regions, where the stability compounds $MgAl_2O_4$ and Al_4C_3 are formed due to low amounts of $CaCO_3$ and Al_2O_3; however, when the amounts of these components are increased, the compound $CaAl_4O_7$ is formed.

Figs. 9 and 10 show the stability phase diagrams at 1073 and 1173 K, respectively. It was observed the formation of two additional regions when the temperature was increased; these are constituted by the stability compounds $MgAl_2O_4$, Al_4C_3, Al_4O_4C and $MgAl_2O_4$, Al_4C_3, Al_4O_4C, $CaAl_4O_7$. These two new regions include the formation of the compound Al_4O_4C and are increased when the temperature was increased from 1073 to 1173 K. The three stabil-

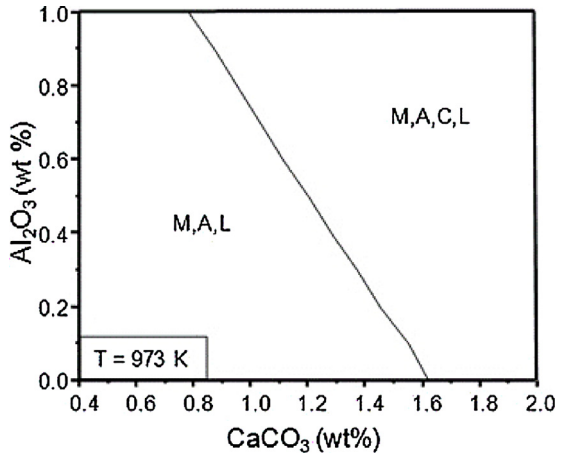

Fig. 8. Stability phase diagram of the $[Al\text{-}Mg]_{alloy}$-$(xAl_2O_3)_{thickening\ agent}$-$(xCaCO_3)_{foaming\ agent}$ at 973 K. (M) $MgAl_2O_4$; (A) Al_4C_3; (C) $CaAl_4O_7$ and (L) Liquid phase.

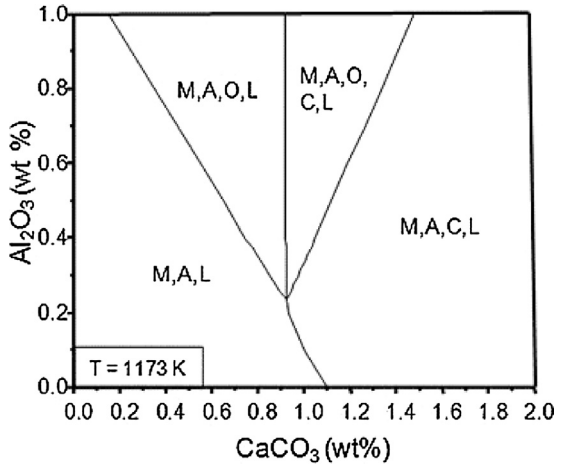

Fig. 9. Stability phase diagram of the $[Al\text{-}Mg]_{alloy}$-$(xAl_2O_3)_{thickening\ agent}$-$(xCaCO_3)_{foaming\ agent}$ at 1073 K. (M) $MgAl_2O_4$; (A) Al_4C_3; (C) $CaAl_4O_7$, (O) Al_4O_4C and (L) Liquid phase.

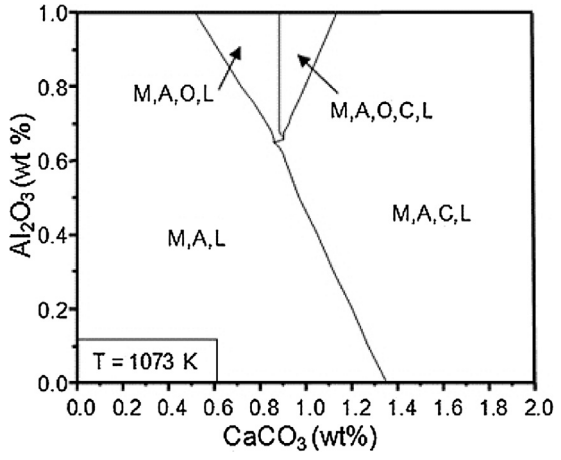

Fig. 10. Stability phase diagram of the $[Al\text{-}Mg]_{alloy}$-$(xAl_2O_3)_{thickening\ agent}$-$(xCaCO_3)_{foaming\ agent}$ at 1173 K. (M) $MgAl_2O_4$; (A) Al_4C_3; (C) $CaAl_4O_7$, (O) Al_4O_4C and (L) Liquid phase.

ity phase diagrams obtained show that the compounds formed are contained in a liquid phase constituted by the molten alloy.

4. Discussion

The closed-cell foams produced showed that the best bubble stability in the melt was obtained for the addition of 1 wt % $CaCO_3$ (Fig. 3a) while an increase in the foaming agent addition, decreased the bubble stability promoting a reduction of the cell wall size, the bubble collapse and finally the breaking of cell walls (Fig. 3c). It was observed an excessive oxidation on the top part of the melt for the foams produced with the higher $CaCO_3$ amounts, affecting its expansion rate. The characteristics and properties of the foams produced by adding $CaCO_3$ as a foaming agent showed an increase of the density and relative density, while the porosity decreased with the increase of the $CaCO_3$ amount, as can be observed in Table 1. The relative density increases and the cell wall size decreases when the $CaCO_3$ amount was increased. Lázaro et al. [7] reported relative densities in the range from 0.15 to 0.25 for the carbonate content from 1 to 3 wt. % which are similar to those obtained in this work. In addition, they reported [7] that for higher carbonate content (>3 wt. %), the foams showed excessive oxidation on the top part, affecting the expansion rate and the stability. Both behaviors were also shown by the foam produced adding 3 wt. % $CaCO_3$ in this work.

The SEM-EDS analysis reported in Figs. 4 to Figure 6 showed a non-homogeneous microstructure of the foams formed by an A356 aluminum alloy matrix with a lot of foreign particles such as Al_2O_3, $CaCO_3$, $CaAl_4O_7$, Al_4O_4C and, Al_4C_3. These particles may correspond to compounds formed by the reaction between the thickening and the foaming agent, or reactions between these two agents with the components in the melt. $CaCO_3$ particles correspond to unreacted $CaCO_3$ or partially reacted particles that could not be retained for the melt, especially for the addition of 3 wt% $CaCO_3$. Also when the amount of the foaming agent was increased to 2 and 3 wt%, the number of compounds formed was increased. Figs. 5 and 6 show an excess of $CaCO_3$ particles that may increase the oxygen concentration due to its decomposition, which develops compounds like Al_4O_4C and $CaAl_4O_7$. It is evident that these compounds play an important role in the foamability behavior.

The Raman analysis of the cell walls shows the presence of different compounds produced by the reaction between the thickening and the foaming agent. Because of the small quantity of the formed components, Al_4C_3, $CaAl_4O_7$ and, $MgAl_2O_4$ Raman signals are barely detected; they are perceived only to the foam obtained with the addition of 2 wt% $CaCO_3$. However, the Al_4O_4C compound is formed under all studied conditions as it can be clearly observed from Raman spectra while calcite quantity strongly increases with $CaCO_3$ wt% addition.

The thermodynamic analysis considered a liquid Al-Mg alloy in contact with a thickening agent (Al_2O_3) which is added on the top of the molten alloy to increase viscosity and then a foaming agent ($CaCO_3$) is added to carry out the foaming process. During the foaming process, the interaction between the alloy and the foaming and thickening agents promotes the compound formation. Therefore, the foaming process could be explained by the following mechanism. The first reaction to take place is the thermal decomposition of the $CaCO_3$ into the molten alloy.

$$CaCO_3 = CaO + CO_2 \quad (2)$$

The magnesium in the molten alloy is highly reactive and reacts with the CO_2 gas released by reaction (2).

$$2Mg + CO_2 = 2\,MgO + C \quad (3)$$

Cochran et al. [26] reported for Al-Mg alloys that after the incubation time crystalline MgO or $MgAl_2O_4$ can nucleate under a

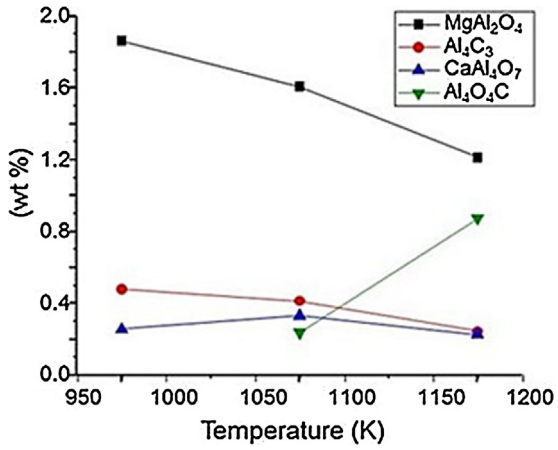

Fig. 11. Effect of the addition of 1% $CaCO_3$ on the phases formed during solidification to the $[Al\text{-}Mg]_{alloy}\text{-}(xAl_2O_3)_{thickening\ agent}\text{-}(1\ wt\%\ CaCO_3)_{foaming}$ system. Lines represent the weight % of each solid phase formed. The balance corresponds to % liquid in the system.

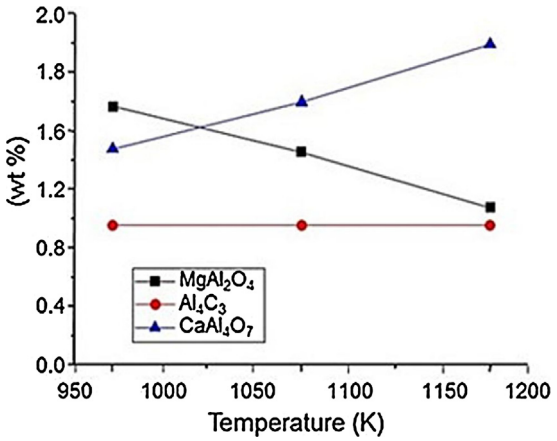

Fig. 12. Effect of the addition of 2% $CaCO_3$ on the phases formed during solidification to the $[Al\text{-}Mg]_{alloy}\text{-}(xAl_2O_3)_{thickening\ agent}\text{-}(1\ wt\%\ CaCO_3)_{foaming}$ system. Lines represent the weight % of each solid phase formed. The balance corresponds to % liquid in the system.

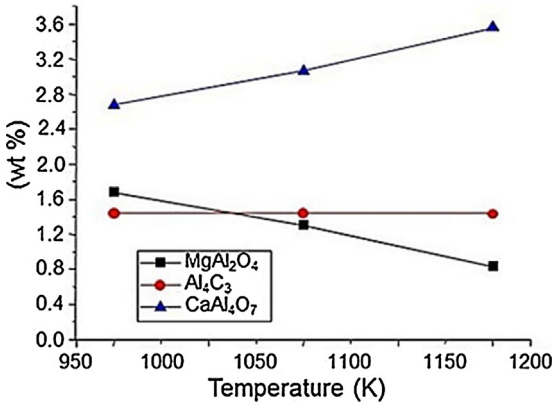

Fig. 13. Effect of the addition of 3% $CaCO_3$ on the phases formed during solidification to the $[Al\text{-}Mg]_{alloy}\text{-}(xAl_2O_3)_{thickening\ agent}\text{-}(1\ wt\%\ CaCO_3)_{foaming}$ system. Lines represent the weight % of each solid phase formed. The balance corresponds to % liquid in the system.

previously formed amorphous MgO film and breakaway oxidation begins, which is ceased only when all the Mg had been oxidized. Therefore, the spinel formation occurs after the MgO has been formed.

The MgO and C formed by reaction (3) react with the thickening agent and with the liquid aluminum to form the spinel ($MgAl_2O_4$) and aluminum carbide (Al_4C_3), respectively, based on reactions ((4) and (5))

$$Al_2O_3 + MgO = MgAl_2O_4 \quad (4)$$

$$4Al + 3C = Al_4C_3 \quad (5)$$

Wightman and Fray reported [27] that different oxides can be formed on the aluminum surface depending on the Mg concentration. They determined the spinel formation experimentally and thermodynamically at 0.59 wt% and 0.34 wt% Mg, respectively. On the other hand, Babcsán [19] determined a minimum amount of $7.9\,10^{-3}$ mol% Mg (0.19 wt %) to form the spinel, which is in good agreement with the magnesium content considered in this analysis (0.38 wt% Mg).

The formation of aluminum carbide (Al_4C_3) is detrimental to composite properties because of its brittleness. The presence of low amounts of magnesium (~1 wt% Mg) in pure aluminum leads to the formation of aluminum carbide [28].

The calcium oxide formed by reaction (2) reacts with the thickening agent to form the $CaAl_4O_7$ compound

$$CaO + 2Al_2O_3 = CaAl_4O_7 \quad (6)$$

The compound Al_4O_4C was formed to high oxidizing conditions; these are obtained when the amount of $CaCO_3$ and the temperature are increased. Therefore, the liquid aluminum reacts with the carbon formed when reaction (3) proceeds and the oxygen from the atmosphere or the CO_2 released by the $CaCO_3$ thermal decomposition.

$$4Al + C + 2O_2 = Al_4O_4C \quad (7)$$

Fig. 11 shows the amounts of compound formation for an addition of 1 wt % $CaCO_3$ to the three temperatures evaluated. It can be shown that the $MgAl_2O_4$ compound was formed in higher amount than the Al_4C_3 and $CaAl_4O_7$ compounds to 973 K. When the temperature was increased, the amount of Al_4C_3, $CaAl_4O_7$ and $MgAl_2O_4$ decreased and the Al_4O_4C compound was formed to 1073 K. The amount of this new compound was increased when the temperature was increased from 973 to 1073 K.

Figs. 12 and 13 show the amounts of compound formation for an addition of 2 and 3 wt % $CaCO_3$ to the three temperatures evaluated, respectively. It is observed that the $MgAl_2O_4$ compound was consumed when the temperature was increased while the amount of the Al_4C_3 compound remained constant and the amount of the $CaAl_4O_7$ compound was increased. For these high $CaCO_3$ additions, there was no evidence of the Al_4O_4C compound, as can be observed in Figs. 9 and 10; the stability region of the Al_4O_4C compound is closer to 1 wt% $CaCO_3$.

Figs. 11 to Figure 13 showed an increase in the amount of the compounds Al_4C_3 and $CaAl_4O_7$ due to the consumption of the $MgAl_2O_4$ compound when the amount of foaming agent was increased. The thermodynamic analysis confirms the presence of the compounds: Al_4C_3, $CaAl_4O_7$ and, Al_4O_4C detected experimentally. The compound Al_4O_4C was experimentally detected to the three $CaCO_3$ additions, while the thermodynamic software determined the formation of this compound to the addition of 1 wt % $CaCO_3$ at 1073 and 1173 K. The $MgAl_2O_4$ compound was determined by the thermodynamic software for the three $CaCO_3$ additions; however, the Raman results showed its presence at 2 wt% $CaCO_3$. The results of the thermodynamic analysis show a good fit with those obtained experimentally.

The compounds $CaAl_4O_7$, Al_4O_4C and, Al_4C_3 determined in this work are known as ceramic or refractory materials that exhibit typical properties, such as a high melting point, high hardness and

brittle behavior which are detrimental to the foam's mechanical properties. In order to decrease the brittle behavior of the closed foams obtained, the foaming process required low amounts of $CaCO_3$ in order to decrease the amount of the compounds formed and decrease the temperature of the foaming process; however, this last consideration depends on the melting temperature of the alloy and the thermal decomposition temperature of the foaming agent. For this work, the thermal decomposition of $CaCO_3$ occurs in the range from 956 K to 1082 K where CO_2 gas is released. In addition, the melting point of the A356 alloy was determined to be at 888 K. Therefore, the foaming process temperature was attained at 1023 K in order to release CO_2 gas into the molten alloy.

5. Conclusions

Stability phase diagrams were obtained to 973, 1073 and 1173 K for the production of the closed-cell A356 aluminum alloy by adding $CaCO_3$ and Al_2O_3 as a foaming and thickening agents, respectively. The compounds $MgAl_2O_4$, $CaAl_4O_7$, Al_4C_3 and Al_4O_4C were predicted by the thermodynamic software. The thermal decomposition of the foaming agent promotes the magnesium oxidation of the alloy and furthermore the $CaAl_4O_7$, Al_4C_3 and, Al_4O_4C compound formation. When the amount of the foaming agent was increased, the amount of the $CaAl_4O_7$, Al_4C_3 compounds was increased. The increase of the temperature promotes the Al_4O_4C compound formation for an addition of 1 wt % $CaCO_3$. The closed-cell foams of the A356 aluminum alloy produced showed the formation of $CaAl_4O_7$, Al_4O_4C and Al_4C_3 compounds which are in good agreement with the compounds predicted by the thermodynamic analysis.

Acknowledgements

The authors wish to thank the Institutions CONACyT, SNI, COFAA and SIP-Instituto Politécnico Nacional for their permanent assistance to the Process Metallurgy Group at ESIQIE-Metallurgy and Materials Department.

References

[1] Davies GJ, Zhen S. Metallic foams: their production, properties and applications. J Mater Sci 1983;18:1899–911.
[2] Dukhan N. Metal foams, fundamentals and applications. first ed. Pennsylvania: Destech Publications Inc.; 2013.
[3] Jin I, Kenny LD, Sang H. US Patent 5112697. 1992.
[4] Akiyama S, Ueno H, Imagawa K, Kitahara A, Nagata S, Morimoto K, Nishikawa T, Itoh M. US Patent 4713277. 1987.
[5] Nakamura T, Gnyloskurenko S, Sakamoto K, Byakova A, Ishikawa R. Development of new foaming agent for metal foam. Mater Trans 2002;43(5):1191–6.
[6] Koizumi T, Kido K, Kita K, Mikado K, Gnyloskurenko S, Nakamura T. Foaming agents for powder metallurgy production of aluminum foam. Mater Trans 2011;52(4):728–333.
[7] Lázaro J, Solorzano E, Rodríguez MA. Alternative carbonates to produce aluminum foams via melt route. Procedia Mater Sci 2014;4:275–80.
[8] Papadopoulos D, Omar H, Stergioudi F, Tsipas S, Michailidis N. A novel method for producing Al-foams and evaluation on their compression behavior. J Porous Mater 2010;17:773–7.
[9] Fernandes H, Tulyaganov D, Ferreira J. Preparation and characterization of foams from sheet glass and fly ash using carbonates as foaming agents. Ceram Int 2009;35:229–35.
[10] Banhart J. Metal foams: production and stability. Adv Eng Mater 2006;8(9):781–94.
[11] Babcsán N, Leitlmeier D, Degischer H. Foamability of particle reinforced aluminum melt. Mat-wiss u Werkstofftech 2003;34:22–9.
[12] Miyoshi T, Itoh M, Akiyama S, Kitahara A. Alporas aluminum foam: production process, properties and, applications. Adv Eng Mater 2002;2(4):735–40.
[13] Yang C, Nakae H. The effects of viscosity and cooling conditions on the foamability of aluminum alloy. J Mater Process Technol 2003;141:202–6.
[14] Fukui T, Nonaka Y, Suzuki S. Fabrication of Al-Cu-Mg alloy foams using Mg as thickener through melt route and reinforcement of cell walls by heat treatment. Procedia Mater Sci 2014;4:33–7.
[15] Simone AE, Gibson LJ. Aluminum foams produced by liquid-state processes. Acta Mater 1998;46(9):3109–23.
[16] Ip SW, Wang Y, Toguri JM. Aluminium foam stabilization by solid particles. Can Metall Q 1999;38(1):81–92.
[17] Byakova A, Kartuzov I, Nakamura T, Gnyloskurenko S. The role of foaming agent and processing route in mechanical performance of fabricated aluminum foams. Procedia Mater Sci 2014;4:109–14.
[18] ALCAN: World Patent WO9317139. 1993.
[19] Babcsán N. Ceramic particles stabilized aluminum foams. PhD Thesis Miskolc Mat Sci Technol School Kerpely Antal 2003.
[20] Bale CW, Pelton AD, Thompson WT. Facility for the analysis of chemical thermodynamics (Factsage 7.0). User's guide; 2016.
[21] Sun Y, Chen Y, Ding C, Yang G, Ma Y, Wang C. One-dimensional Al_4O_4C ceramics: A new type of blue light emitter. Sci Rep 2013;3:1–6.
[22] Yang L, Tan Z, Ji G, Li Z, Fan G, Schryvers D, et al. A quantity method to characterize the Al_4C_3-formed interfacial reaction: the case study of MWCNT/Al composites. Mater Charact 2016;112:213–8.
[23] Hofmeister AM, Wopenka B, Locock AJ. Spectroscopy and structure of hibonite, grossite, and $CaAl_2O_4$: implications for astronomical environments. Geochim et Cosmochim Acta 2004;68(21):4485–503.
[24] Minh NV, Yang IS. A Raman study of cation-disorder transition temperature of natural $MgAl_2O_4$ spinel. Vib Spectrosc 2004;35:93–6.
[25] Falgayrac G, Sobanska S, Brémard C. Raman diagnostic of the reactivity between $ZnSO_4$ and $CaCO_3$ particles in humid air relevant to heterogeneous zinc chemistry in atmosphere. Atmos Environ 2014;85:83–91.
[26] Cochran C, Belitskus D, Kinosz D. Oxidation of Al-Mg melts in air, oxygen, flue gas and carbon dioxide. Metall Mater Trans B 1977;8:323–32.
[27] Wightman G, Fray D. The dynamic oxidation of aluminum and its alloys. Metall Trans B 1983;14:625–31.
[28] Cayron C. EMPA report No 250, Thun, Switzerland. 2001.